British Journal of Pharmacology

DOI:10.1111/j.1476-5381.2011.01285.x
www.brjpharmacol.org

RESEARCH PAPER

Pharmacological characterization of GSK1004723, a novel, long-acting antagonist at histamine H_1 and H_3 receptors

RJ Slack[1], LJ Russell[1], DA Hall[1], MA Luttmann[3], AJ Ford[1], KA Saunders[1], ST Hodgson[2], HE Connor[1], C Browning[1] and KL Clark[1]

[1]*Respiratory Biology and* [2]*Medicinal Chemistry, Respiratory CEDD, GlaxoSmithKline, Stevenage, UK, and* [3]*Respiratory Biology, Respiratory CEDD, GlaxoSmithKline, King of Prussia, PA, USA*

Correspondence
KL Clark, Respiratory CEDD, GlaxoSmithKline Medicines Research Centre, Gunnels Wood Road, Stevenage, Hertfordshire, SG1 2NY, UK. Email: kenneth.i.clark@gsk.com

Keywords
allergic rhinitis; duration of action; GSK1004723; histamine antagonist; histamine H_1 receptor; histamine H_3 receptor; human; long-acting; non-clinical

Received
9 July 2010
Revised
13 January 2011
Accepted
8 February 2011

BACKGROUND AND PURPOSE
Preclinical pharmacological characterization of GSK1004723, a novel, dual histamine H_1 and H_3 receptor antagonist.

EXPERIMENTAL APPROACH
GSK1004723 was characterized *in vitro* and *in vivo* using methods that included radioligand binding, intracellular calcium mobilization, cAMP production, GTPγS binding, superfused human bronchus and guinea pig whole body plethysmography.

KEY RESULTS
In cell membranes over-expressing human recombinant H_1 and H_3 receptors, GSK1004723 displayed high affinity, competitive binding (H_1 p*Ki* = 10.2; H_3 p*Ki* = 10.6). In addition, GSK1004723 demonstrated slow dissociation from both receptors with a $t_{1/2}$ of 1.2 and 1.5 h for H_1 and H_3 respectively. GSK1004723 specifically antagonized H_1 receptor mediated increases in intracellular calcium and H_3 receptor mediated increases in GTPγS binding. The antagonism exerted was retained after cell washing, consistent with slow dissociation from H_1 and H_3 receptors. Duration of action was further evaluated using superfused human bronchus preparations. GSK1004723 (100 nmol·L^{-1}) reversed an established contractile response to histamine. When GSK1004723 was removed from the perfusate, only 20% recovery of the histamine response was observed over 10 h. Moreover, 21 h post-exposure to GSK1004723 there remained almost complete antagonism of responses to histamine. *In vivo* pharmacology was studied in conscious guinea pigs in which nasal congestion induced by intranasal histamine was measured indirectly (plethysmography). GSK1004723 (0.1 and 1 mg·mL^{-1} intranasal) antagonized the histamine-induced response with a duration of up to 72 h.

CONCLUSIONS AND IMPLICATIONS
GSK1004723 is a potent and selective histamine H_1 and H_3 receptor antagonist with a long duration of action and represents a potential novel therapy for allergic rhinitis.

Abbreviations
$Al(OH)_3$, aluminium hydroxide; ANOVA, one-way analysis of variance; B_{max}, total number of receptors; Ca^{2+}, calcium; cAMP, 3′-5′-cyclic adenosine monophosphate; Carbachol, carbamylcholine; CHO-K1, Chinese hamster ovary; Clobenpropit, clobenpropit dihydrochloride; CRC, concentration response curve; DMSO, dimethyl sulphoxide; EDTA, eythlenediaminetetraacetic acid; FLIPR, fluorometric imaging plate reader; GSK1004723, 4-[(4-Chlorophenyl)methyl]-2-({(2*R*)-1-[4-(4-{[3-(hexahydro-1H-azepin-1-yl)propyl]oxy}phenyl)butyl]-2-pyrrolidinyl}methyl)-1(2*H*)-phthalazinone; H_1, histamine-1; H_2, histamine-2; H_3, histamine-3; H_4, histamine-4; HBSS, Hank's buffered salt solution; HEK293, human embryonic kidney; HEPES, N-2-hydroxyethylpiperazine-N′-ethanesulphonic acid; [^{3}H]-GSK189254, tritiated 6-[(3-Cyclobutyl-2,3,4,5-tetrahydro-1*H*-3-benzazepin-7-yl)oxy]-*N*-methyl-3-pyridinecarboxamide hydrochloride;

[^{3}H]-mepyramine, [pyridinyl-5-^{3}H]Pyrilamine; K_D, equilibrium dissociation constant; K_i, inhibition constant; K_{obs}, observed rate constant; k_{off}, dissociation rate; k_{on}, association rate; LS, liquid scintillation; Mepyramine, pyrilamine maleate; NSB, non-specific binding; OVA, ovalbumin; pA_2, apparent antagonist potency; PBS, phosphate buffered saline; PenH, enhanced pause; PMSF, phenylmethylsulphonyl fluoride; SEM, standard error of the mean; [^{35}S]GTPγS, guanosine 5′-O-(3-[^{35}S]thio)triphosphate; $t_{1/2}$, half-life

Introduction

Allergic rhinitis is a highly prevalent disease estimated to impact around 10–20% of the population (Passalacqua and Ciprandi, 2006; Al Suleimani and Walker, 2007). Importantly, this condition continues to have an impact on patient quality of life and also carries a significant economic burden (Schoenwetter *et al.*, 2004; Borres, 2009). Although many treatment options are available, current therapies for allergic rhinitis remain suboptimal with respect to either speed of onset, duration of action and/or ability to suppress all key symptoms of the disease. For example, histamine-1 (H_1) receptor antagonists are effective in relieving rhinorrhoea, itching and sneezing but have limited efficacy on nasal congestion (Spector, 1999; Al Suleimani and Walker, 2007; Meltzer *et al.*, 2010). Similarly, previous workers have found that the increase in nasal congestion provoked by nasal histamine challenge is only partially blunted by H_1 and histamine-2 (H_2) receptor antagonists (Wood-Baker *et al.*, 1996; Howarth, 1997). These findings have led us and others in the field to consider whether other subtypes of histamine receptor may contribute to the histamine-induced nasal congestion. A growing body of evidence suggests that the histamine-3 (H_3) receptor may play a role.

H_3 receptors were first described at a molecular level in 1999 (Lovenberg *et al.*, 1999) and are highly and preferentially expressed in the CNS where they play a role as autoreceptors (Arrang *et al.*, 1983; Leurs *et al.*, 2005). However, H_3 receptors are also expressed in the periphery where they appear to play a role in regulating the peripheral autonomic system. In 2004, two groups (Nakaya *et al.*, 2004; Varty *et al.*, 2004) discovered evidence for the expression of the H_3 receptor in human nasal mucosa. Furthermore, Varty *et al.* (2004) demonstrated that in human nasal mucosa, activation of H_3 receptors appeared to inhibit sympathetically mediated contractile responses, leading to the hypothesis that H_3 receptors, via this mechanism, may contribute to dilation of nasal blood vessels and nasal congestion. This hypothesis gained support following a clinical investigation (Taylor-Clark *et al.*, 2005) which also demonstrated that in healthy volunteers, histamine-induced nasal congestion was more significantly attenuated by combined H_1 and H_3 receptor blockade, relative to H_1 and H_3 receptor blockade in isolation. Together with similar findings from a preclinical model of nasal congestion (McLeod *et al.*, 1999), this study strengthened the hypothesis that H_3 receptors contribute to histamine-induced nasal congestion and also indicate that to have a significant impact on this important symptom of rhinitis, it may be necessary to simultaneously block both H_1 and H_3 receptors (Taylor-Clark and Foreman, 2005). Based on this evidence and recognizing the need for new treatment options in rhinitis, we initiated a drug discovery programme to identify a dual H_1 and H_3 receptor antagonist with a profile suitable for once a day dosing.

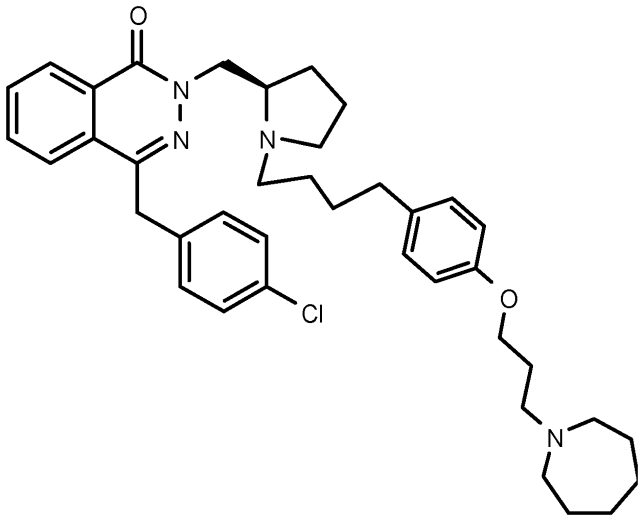

Figure 1
The structure of the H_1 and H_3 receptor antagonist GSK1004723.

Given uncertainty over the tolerability of H_3 receptor blockade in non-nasal peripheral tissues and in the CNS, the programme focused in part on the discovery of a molecule which could be delivered topically via the intranasal route. To obtain a long duration of action with intranasally delivered molecules, it is important to focus on the optimal combination of physiochemical characteristics, potency and receptor kinetics. This manuscript describes the pharmacological characteristics of 4-[(4-Chlorophenyl)methyl]-2-({(2*R*)-1-[4-(4-{[3-(hexahydro-1*H*-azepin-1-yl)propyl]oxy}phenyl)butyl]-2-pyrrolidinyl}methyl)-1(2*H*)-phthalazinone (GSK1004723) (Figure 1), a novel dual H_1 and H_3 receptor antagonist with a long duration of action potentially consistent with once a day, intranasal, clinical dosing.

Methods

In vitro

Cell culture and membrane preparation. Chinese hamster ovary (CHO-K1) cells were stably transfected with the human H_1 receptor as previously described (Smit *et al.*, 1996). The cells were grown in T175 cm^2 flasks or 1800 cm^2 roller bottles at 37°C in a 95% O_2/5% CO_2 atmosphere in growth medium (α-minimal essential medium without ribonucleotides and deoxyribonucleotides containing 10% dialysed fetal bovine serum and 200 mmol·L^{-1} L-glutamine).

Human embryonic kidney (HEK293) cells were transfected with the human H_2 receptor using the BacMam viral

transduction method (Kost and Condreay, 2002). The cells were grown in T175 cm^2 flasks at 37°C in a 95% O_2/5% CO_2 atmosphere in growth medium (FreeStyle™ 293 Expression Medium).

The CHO-K1 cells were stably transfected with the human H_3 receptor under a GeneSwitch™ inducible promoter. The cells were grown in T175 cm^2 flasks or 1800 cm^2 roller bottles at 37°C in a 95% O_2/5% CO_2 atmosphere in growth medium (Ham's F12 medium containing 10% fetal bovine serum, 200 mmol·L^{-1} L-glutamine, 0.2 mg·mL^{-1} hygromycin-B and 0.25 mg·mL^{-1} zeocin).

The HEK293 cells were stably transfected with the human histamine-4 (H_4) receptor (Liu *et al.*, 2001). The cells were grown in T175 cm^2 flasks at 37°C in a 95% O_2/5% CO_2 atmosphere in growth medium (Dulbecco's modified Eagles medium containing 10% fetal bovine serum).

For preparation of H_1, H_2 and H_3 membranes, cells were harvested from confluent 1800 cm^2 roller bottles following treatment with Hank's buffered salt solution (HBSS) containing 0.6 mmol·L^{-1} eythlenediaminetetraacetic acid (EDTA) and centrifugation at 250× *g* for 5 min. The pellet was suspended in HBSS containing 0.6 mmol·L^{-1} EDTA and centrifuged again at 250× *g* for 5 min. The pellet was suspended in homogenization buffer [mmol·L^{-1}: N-2-hydroxyethylpiperazine-N'-ethanesulphonic acid (HEPES), 50.0; bacitracin, 25 µg·mL^{-1}; EDTA, 1.0; leupeptin, 0.1; phenylmethylsulphonyl fluoride (PMSF), 1.0; Pepstatin A, 0.002; pH 7.4], placed on ice for 5 min and then homogenized in a glass Waring blender for 2 × 15 s bouts at 4°C. The homogenate was centrifuged at 500× *g* for 20 min at 4°C and the resulting supernatant was centrifuged at 48 000× *g* for 36 min at 4°C. The supernatant was discarded and the pellet suspended in homogenization buffer (without PMSF and Pepstatin A). The membrane suspension was then forced through a 0.6 mm needle and frozen in aliquots at –80°C until required. The protein concentration was determined by the Bradford method (Bradford, 1976) using bovine serum albumin as a standard. H_4 cell membranes were prepared as previously described by Liu *et al.* (2001).

Biochemical assays. H_2 3'-5'-cyclic adenosine monophosphate (cAMP) accumulation assays were performed in white, 384-well plates at ambient room temperature (20–22°C) in assay buffer (mmol·L^{-1}: HEPES, 50; 3-isobutyl-1-methylxanthine, 2.2 µg·mL^{-1}; $MgCl_2$, 10; NaCl, 100; pH 7.4). 10 µL H_2 membranes (3 µg·$well^{-1}$) and 0.5 µL of antagonist/vehicle [in 100% dimethyl sulphoxide (DMSO) to give a final concentration of 2.5% DMSO] at varying concentrations were incubated for 20 min prior to addition of 10 µL assay buffer containing 0.6 mmol·L^{-1} adenosine-5'-triphosphate and 4 µmol·L^{-1} histamine (EC_{80} concentration). Following a further 30 min incubation, cAMP accumulation was measured with a cAMP enzyme fragment complementation assay (Hithunter™ cAMP (90-0004L), DiscoveRx Corporation Ltd, Fremont, CA, USA) following the manufacturer's instructions.

H_3 Guanosine 5'-O-(3-[^{35}S]thio)triphosphate ([^{35}S]GTPγS) binding studies were performed in 96-deep well plates at 30°C in assay buffer (mmol·L^{-1}: HEPES, 20; NaCl, 100; $MgCl_2$, 10; guanosine 5'-diphosphate, 0.01; saponin, 10 µg·mL^{-1}; pH 7.4). In total, 200 µL H_3 membranes (10 µg·$well^{-1}$), 25 µL histamine and 25 µL antagonist/vehicle were incubated for 30 min prior to addition of 10 µL [^{35}S]GTPγS (~0.1 nmol·L^{-1}). Following a further 30 min incubation, reactions were terminated by rapid vacuum filtration through a 48-well Brandel (Brandel Inc., Gaithersburg, MD, USA) harvester onto GF/B filter papers. Samples were washed rapidly three times with 1 mL ice-cold distilled water and transferred to liquid scintillation (LS) vials containing 4 mL of LS fluid. [^{35}S]GTPγS bound was measured by LS spectroscopy using a Wallac 1409 DSA LS counter (PerkinElmer LAS UK Ltd, Beaconsfield, UK).

Measurement of intracellular calcium (Ca^{2+}) mobilization. CHO-H_1 and H_3 cells were grown to confluency in T175 cm^2 flasks and harvested by treatment with versene for 10 min at 37°C followed by centrifugation at 350× *g* for 5 min. Cell pellets were suspended in the respective H_1 or H_3 growth medium (containing 100 nmol·L^{-1} mifepristone for CHO-H_3 cells) and seeded into tissue culture treated, black, 96-well clear bottomed, fluorometric imaging plate reader (FLIPR) plates (200 µL, 60 000 cells per well) and incubated at 37°C for 16 h. Growth medium was aspirated and cells gently washed (200 µL) with phosphate buffered saline (PBS) (mmol·L^{-1}: NaCl, 137.0; Na_2HPO_4, 8.1; KCl, 2.7; KH_2PO_4, 1.5; $CaCl_2$, 0.9; $MgCl_2$, 0.5). Subsequent methodology was dependent on experiment type (as detailed below) and FLIPR assay buffer consisted of 0.5 mmol·L^{-1} brilliant black (ICN Biomedicals, Irvine, CA, USA) made up in Tyrode's buffer (mmol·L^{-1}: NaCl, 145; HEPES, 10.0; D-glucose, 10.0; KCl, 5.0; $CaCl_2$, 0.8; pH 7.4).

For CHO-H_1 Schild analysis, PBS was aspirated from CHO-H_1 cells and loading buffer (assay buffer containing 2.5 mmol·L^{-1} probenecid and 2 µmol·L^{-1} Fluo-4 AM Ca^{2+} dye) added to cells (50 µL) and incubated at 37°C for 45 min. Loading buffer was aspirated and cells gently washed (200 µL) in PBS before addition of assay buffer (90 µL). Antagonist/vehicle test solutions prepared in assay buffer were added to cells (10 µL) and incubated at 37°C for either 0.5 or 4 h. Concentration response curves (CRCs) for histamine (prepared in assay buffer) were added to cells (50 µL) following antagonist/vehicle incubation and fluorescence measured.

For CHO-H_1 and H_3 duration of action studies, PBS was aspirated from cells and Tyrode's buffer added (90 µL). Antagonist CRCs and vehicle test solutions were prepared in Tyrode's buffer, added to cells (10 µL) and incubated at 37°C for 30 min. Test solutions were aspirated and cells gently washed (200 µL) twice in PBS. Loading buffer was added to cells (100 µL) and incubated at 37°C for 45 min. Cells were then challenged with a single concentration of histamine (CHO-H_1 – 40 nmol·L^{-1}; CHO-H_3 – 3.3 µmol·L^{-1}) and fluorescence measured. For measuring the reversibility of H_1 and H_3 antagonists, the same method was used with a re-equilibration step incorporated. Following aspiration of test solutions, cells were washed twice in PBS (200 µL), Tyrode's buffer added (100 µL), and cells allowed to re-equilibrate (3 and 4.5 h for CHO-H_1 and CHO-H_3 cells respectively). Cells were then washed twice in PBS (200 µL) before continuation of the method described above.

Cell fluorescence (λ_{ex} = 488 nm and λ_{em} = 518 nm) was measured using a FLIPR (Molecular Devices Ltd, Wokingham, UK) before and after addition of histamine challenge for 60 s. The histamine stimulated increase in fluorescence was determined by subtracting the basal fluorescence from the peak

fluorescence response following histamine addition. This value was then expressed as a percentage increase in basal fluorescence.

Radioligand binding assays

General protocols for H_1 and H_3 binding assays. All H_1 and H_3 radioligand binding assays were performed in 96-deep well plates at 37°C in assay buffer (50 mmol·L^{-1} HEPES; pH 7.4) with 50 µL radioligand, 400 µL membranes (20 µg·well^{-1} H_1 and 2.5 µg·well^{-1} H_3) and 50 µL of either vehicle or unlabelled antagonist at varying concentrations. For H_1 binding studies, [pyridinyl-5-^{3}H]Pyrilamine ([^{3}H]-mepyramine) was used as the radioligand and for H_3, tritiated 6-[(3-Cyclobutyl-2,3,4,5-tetrahydro-1*H*-3-benzazepin-7-yl)oxy]-*N*-methyl-3-pyridinecarboxamide hydrochloride ([^{3}H]-GSK189254) (Medhurst *et al.*, 2007). Plates were incubated with gentle agitation for the time periods indicated. Non-specific binding (NSB) was determined in the presence of either 10 µmol·L^{-1} azelastine (H_1) or clobenpropit (H_3). Radioligand binding was terminated by rapid vacuum filtration through a 48-well Brandel harvester onto GF/B filter papers pre-soaked in 0.3% v/v poly-ethylenimine. Samples were washed rapidly three times with 1 mL ice-cold distilled water and transferred to LS vials containing 4 mL of LS fluid. The amount of radioligand bound to receptor was measured by LS spectroscopy. By the same method the concentration of total radioligand added to each well was calculated for data analysis and also to ensure that <10% of radioligand was bound, thus preventing issues associated with depletion of free radioligand in the system (Hulme and Birdsall, 1992).

Radioligand characterization. Saturation, association and dissociation binding studies were performed for [^{3}H]-mepyramine and [^{3}H]-GSK189254 to determine receptor binding kinetics at H_1 and H_3, respectively (equilibrium dissociation constant (K_D), total number of receptors (B_{max}), association rate (k_{on}) and dissociation rate (k_{off}) were calculated as described under *Data analysis and statistics*). For saturation binding, membranes (in a volume of 1.4 mL to avoid ligand depletion) were incubated with increasing concentrations of radioligand (~0.02–28 nmol·L^{-1} for [^{3}H]-mepyramine and ~0.005–4 nmol·L^{-1} for [^{3}H]-GSK189254) for 1 h prior to filtration. For association binding, membranes were incubated with different concentrations of radioligand (~1–11 nmol·L^{-1} for [^{3}H]-mepyramine and ~0.3–3 nmol·L^{-1} for [^{3}H]-GSK189254) for varying incubation times up to 10 min prior to filtration. For dissociation binding, membranes were pre-incubated for 1 h with a fixed concentration of radioligand (~2 nmol·L^{-1} for [^{3}H]-mepyramine and ~0.6 nmol·L^{-1} for [^{3}H]-GSK189254) before addition of cold ligand (10 µmol·L^{-1} of either azelastine or GSK1004723 for H_1 and clobenpropit or GSK1004723 for H_3) and incubation for varying times up to 10 min prior to filtration.

Determination of antagonist affinity and competition kinetics. In order to determine the affinity of antagonists, competition binding displacement studies were completed where membranes were incubated with a fixed concentration of radioligand (~6 or 0.8 nmol·L^{-1} for H_1 and H_3 respectively) and increasing concentrations of unlabelled antagonist for 5 h prior to filtration. H_4 radioligand competition binding assays were performed by CEREP screen (Paris, France) using a protocol previously described (Liu *et al.*, 2001).

For competition kinetics studies the effects of unlabelled antagonists on [^{3}H]-mepyramine and [^{3}H]-GSK189254 association to H_1 and H_3 receptors, respectively, were measured. H_1 and H_3 membranes were incubated with a fixed concentration of radioligand (~6 or 0.8 nmol·L^{-1} for H_1 and H_3 respectively) and either vehicle or unlabelled antagonist (three different concentrations tested to ensure k_{on} and k_{off} values determined were independent of antagonist concentration) for varying incubation times up to 30 min prior to filtration. Data were fitted globally as described under *Data analysis and statistics*.

Duration of action studies using human superfused isolated bronchus. Human lungs from organ donors were obtained from the National Disease Research Interchange (NDRI, Philadelphia, PA, USA) in accordance with local human biological sample management procedures. The human biological samples were sourced ethically and their research use was in accord with the terms of the informed consents. Sections of bronchus were removed from human lung and cleaned of adherent connective, parenchymal and fatty tissue. Bronchial strips of 3–4 mm in width were prepared and placed into modified Kreb's solution (mmol·L^{-1}: NaCl, 113.0; KCl, 4.8; $CaCl_2$, 2.5; KH_2PO_4, 1.2; $MgSO_4$, 1.2; $NaHCO_3$, 25.0; D-glucose, 11.0). Bronchial strips were suspended in superfusion tissue baths connected to an isometric transducer, allowing changes in isometric force to be recorded. The protocol used for the superfusion tissue bath experiments was adapted from methods previously described by Coleman and Nials (1989). Briefly, superfusion tissue baths constantly washed tissues with perfusate [modified Kreb's solution containing meclofenamic acid (1 µmol·L^{-1})] at a rate of 2 mL·min^{-1}, maintained at 37°C and gassed with 95% O_2/5% CO_2. An initial tension of 1.5 g was applied and tissues left to equilibrate for 17–22 h. Cimetidine (1 µmol·L^{-1}) and clobenpropit dihydrochloride (clobenpropit) (1 µmol·L^{-1}) were added to the perfusate for at least 30 min before addition of histamine (10 µmol·L^{-1}). Upon reaching sustained histamine-induced contraction, antagonist or vehicle were infused at a rate of 0.02 mL·min^{-1}, at single concentrations per tissue for 3 h until a sustained level of inhibition was attained (antagonist/vehicle test solutions made up in 100% DMSO and added to perfusate to give a final concentration of 0.1% DMSO). The antagonist/vehicle was then removed from perfusate and histamine-induced tension allowed to recover for 10 h. Following the recovery period histamine was removed from the perfusate and tension allowed to return to basal tone before exposure to 10 µmol·L^{-1} carbamylcholine (carbachol) to measure tissue integrity. A cumulative CRC to histamine was constructed by addition of histamine to the perfusate. The start of the histamine CRC corresponded to a 21 h washout from the removal of antagonist/vehicle from the perfusate. Tissues were then exposed to a final carbachol dose (100 µmol·L^{-1}) to measure integrity and for data normalization.

Data were collected by using the Acq*Knowledge* software package (BIOPAC Systems, Goleta, CA, USA) that measured the maximum tension generated throughout the experiment. For histamine CRCs, data were expressed as a percentage of

the final carbachol-induced contraction. For antagonist duration of action, data were expressed as a percentage of the initial antagonist inhibition of histamine contraction.

In vivo

Duration of action studies using whole body plethysmography. Intranasal histamine challenge in guinea pigs elicits symptoms of rhinitis such as rhinorrhoea and nasal congestion. As this species is an obligate nose breather, these responses to histamine have a significant effect on respiration. Therefore, we developed a guinea pig model of whole body plethysmography where changes in enhanced pause (PenH) were used as a surrogate marker of nasal congestion (Saunders *et al.*, 2007). To build confidence that PenH changes in response to intranasal histamine correlate to a nasal and not a pulmonary effect, we performed a series of background experiments (data not included) showing that the intranasal histamine challenge only affected the nasal passage. First, we demonstrated dose localization, via administration of varying intranasal challenge volumes spiked with Evan's blue dye. These were followed by post-mortem analysis of the nasal cavity and oesophagus/trachea to ensure total nasal coverage but no further progression of the dose. Second, we protected the lower airway by exposing guinea pigs to 100 μmol·L^{-1} nebulized salbutamol, and clearly showed no reversal of histamine induced PenH changes. Therefore, our background work suggests that PenH is a reasonable marker of nasal responses to histamine, most likely reflecting changes in nasal congestion. Testing of GSK1004723 was carried out as follows.

Female Dunkin-Hartley guinea pigs (Harlan Laboratories Inc., Huntington, UK) 150–250 g were intranasally sensitized with ovalbumin (OVA) and aluminium hydroxide ($Al(OH)_3$) as previously described (Saunders *et al.*, 2007). Briefly, all intranasal sensitizing solutions were dissolved in physiological saline and 25 μL administered consciously and bilaterally via Gilson pipette. Following acclimatization, animals were dosed twice daily for the first week (Days 0–4) with 20 μg·mL^{-1} OVA and 180 mg·mL^{-1} $Al(OH)_3$. In subsequent weeks, once daily 5 mg·mL^{-1} OVA was administered (Days 7–11, 14–18 and 21–25) except on days of challenge or compound pretreatment.

Dosing and challenge of guinea pigs was undertaken during days 21–25 of the study. A total of 25 μL of azelastine dihydrochloride (1 mg·mL^{-1} free base), GSK1004723 (0.1 mg·mL^{-1} or 1 mg·mL^{-1} free base) or saline vehicle was administered intranasally and bilaterally under isoflurane anaesthesia at the relevant time point prior to challenge (1 h–168 h). 30 min prior to challenge, atropine monohydrate hemisulphate (1 mg·kg^{-1} intraperitoneal) was administered to assist in preventing complete nasal occlusion during challenge.

Guinea pigs were intranasally challenged (25 μL, bilateral) with either 15 mmol·L^{-1} histamine or PBS vehicle under brief isoflurane anaesthesia. During recovery animals remained supine for 1 min, followed by 9 min on their left flank, before transfer to Buxco® (Wilmington, NC, USA) whole body plethysmography chambers. PenH was then recorded consecutively for 4 × 10 min periods and a cumulative total obtained. Replicates of five to six animals were achieved in the PBS challenged groups and six to 10 animals for each of the histamine challenged cohorts. All animal studies were ethically reviewed and carried out in accordance with Animals (Scientific Procedures) Act 1986 and the GSK Policy on the Care, Welfare and Treatment of Laboratory Animals.

Data analysis and statistics

Analysis of all experiments was completed using Prism 5.0 (GraphPad Software, San Diego, CA, USA). Unless otherwise indicated, data shown graphically are mean ± standard error of the mean (SEM). Histamine CRCs, antagonist competition binding displacement curves, and radioligand saturation binding curves were fitted using non-linear regression analysis [four-parameter logistic equation with variable slope (Hill, 1909)] with EC_{50}, IC_{50} and K_D/B_{max} values, respectively, calculated from the fits. IC_{50} values from antagonist competition binding displacement curves were converted to inhibition constant (K_i) values using the Cheng–Prusoff equation (Cheng and Prusoff, 1973). Schild plots were constructed (as described by Arunlakshana and Schild, 1959) from the analysis of histamine CRCs in the presence and absence of varying concentrations of antagonist. From this analysis apparent antagonist potency (pA_2) and slope values were calculated.

Radioligand k_{off} (min^{-1}) values were calculated from dissociation data fitted to a one phase exponential rate of decay. Observed rate constants (K_{obs}) were calculated from association data fitted to a one phase exponential rate of association. The k_{on} (mol·L^{-1}·min^{-1}) values were then calculated using K_{obs} and k_{off} values in Equation 1.

$$k_{on} = \frac{(K_{obs} - k_{off})}{[\text{radioligand}]} \tag{1}$$

The k_{on} and k_{off} values for unlabelled antagonists were determined by non-linear regression analysis of data generated from competition kinetics as originally described by Motulsky and Mahan (1984). Experimental data were globally fitted to a two-component exponential curve as described by Equation 2.

All parameters were fixed apart from k_3 and k_4, the k_{on} and k_{off} constants, respectively, of the unlabelled antagonist.

$$[RL] = \frac{Nk_1[L]}{K_F - K_S}\left(\frac{k_4(K_F - K_S)}{K_F K_S} + \frac{(k_4 - K_F)}{K_F}\exp(-K_F t) - \frac{(k_4 - K_S)}{K_S}\exp(-K_S t)\right) \tag{2}$$

where,

$$K_F = 0.5\left(K_A + K_B + \sqrt{(K_A - K_B)^2 + 4k_1k_3[L][I]}\right)$$

$$K_S = 0.5\left(K_A + K_B - \sqrt{(K_A - K_B)^2 + 4k_1k_3[L][I]}\right)$$

$$K_A = k_1[L] + k_2$$

$$K_B = k_3[I] + k_4$$

Parameter abbreviations used are: $[L]$ = free radioligand concentration; $[I]$ = free unlabelled antagonist concentration; $[RL]$ = specific radioligand binding; $N = B_{max}$; k_1 = association constant of radioligand; k_2 = dissociation constant of radioligand.

K_D values for unlabelled antagonists were calculated from the individual kinetically derived k_{on} and k_{off} values for each unlabelled antagonist, within each competition kinetics experiment, using Equation 3.

$$K_D = \frac{k_{off}}{k_{on}} \quad (3)$$

Dissociation half-life ($t_{1/2}$) values for unlabelled antagonists were calculated from the individual kinetically derived k_{off} value for each antagonist using Equation 4.

$$t_{1/2} = \frac{0.693}{k_{off}} \quad (4)$$

The $t_{1/2}$-values for antagonist onset and offset in isolated superfused human bronchus were calculated from fitting data to a one phase exponential rate of association or decay respectively.

All statistical analyses were completed on $\log_{10}$ transformed data and differences of $P < 0.05$ were considered to be significant. Statistical significance between two data sets was tested using a Student's unpaired *t*-test. Statistical analysis of cumulative 40 min PenH data was completed using Statistica v8 (Statsoft, Inc., Tulsa, OK, USA). One-way analysis of variance (ANOVA) was used for comparison between datasets and where significance was observed Fisher's tests were undertaken to highlight specific inter-group *P*-values. This was further strengthened by Hochberg *post hoc* analysis to account for multiple (relevant) comparisons being made.

Materials

All cell culture media and reagents were obtained from Gibco (Invitrogen Ltd, Paisley, UK). DMSO, 96-deep well binding plates, T175 cm^2 tissue culture flasks and tissue culture treated 96-well clear bottomed black plates were purchased from Fisher Scientific UK Ltd. (Loughborough, UK). The 1800 cm^2 cell culture roller bottles and white 384-well plates were obtained from Corning Inc. (Corning, NY, USA). GSK1004723, GSK189254 and azelastine were synthesized at GlaxoSmithKline Medicines Research Centre (Stevenage, UK). Clobenpropit was purchased from MP Biomedicals Inc. (Solon, OH, USA). Carbamylcholine chloride, cimetidine, histamine dihydrochloride, meclofenamic acid sodium salt, pyrilamine maleate (mepyramine), atropine monohydrate hemisulphate and all other chemicals were obtained from Sigma-Aldrich Co. Ltd. (Gillingham, UK) unless otherwise stated. [^{3}H]-mepyramine (26 Ci·mmol^{-1} specific activity), LS vials and LS fluid (Ultima-Flo™ M) were purchased from PerkinElmer LAS UK Ltd. (Beaconsfield, UK). [^{3}H]-GSK189254 and [^{35}S]GTPγS (specific activities 82 and ~1000 Ci·mmol^{-1} respectively) were obtained from GE Healthcare UK Ltd. (Little Chalfont, UK). GF/B filter papers were purchased from Alpha Biotech Ltd. (London, UK). All *in vitro* studies were completed with a final DMSO concentration of 1% unless otherwise stated. Drug and molecular target nomenclature conforms to the *British Journal of Pharmacology* Guide to Receptors and Channels (Alexander *et al.*, 2009).

Results

Characterization of radioligand binding in recombinant CHO-H_1 and CHO-H_3 cell membranes

[^{3}H]-mepyramine saturation binding studies were carried out at 37°C to determine the expression level of H_1 receptors in the CHO-H_1 cell line. Using CHO-H_1 cell membrane fragments, the B_{max} determined was 1.11 ± 0.12 pmol·mg^{-1} with a pK_D value of 8.83 ± 0.05 (mean ± SEM, n = 4). In addition, association and dissociation binding studies for [^{3}H]-mepyramine were also completed at 37°C (data not shown). The k_{on} was calculated to be 1.22 ± 0.14 × 10^9 mol·min^{-1} (mean ± SEM, n = 3). The k_{off} was calculated to be 0.83 ± 0.07 min^{-1} (mean ± SEM, n = 7) and 1.04 ± 0.04 min^{-1} (mean ± SEM, n = 4) using 10 µmol·L^{-1} azelastine and GSK1004723 respectively. No significant difference was observed between k_{off} values determined with azelastine and GSK1004723 (Student's unpaired *t*-test). The H_1 receptor binding kinetics data generated for [^{3}H]-mepyramine in this study are in close agreement with historical data (Gillard and Chatelain, 2006).

[^{3}H]-GSK189254 saturation binding studies were carried out at 37°C to determine the expression level of H_3 receptors in the CHO-H_3 cell line. Using CHO-H_3 cell membrane fragments, the B_{max} determined was 5.92 ± 0.42 pmol·mg^{-1} with a pK_D value of 9.72 ± 0.04 (mean ± SEM, n = 4). In addition, association and dissociation binding studies for [^{3}H]-GSK189254 were also completed at 37°C (data not shown). The k_{on} was calculated to be 5.58 ± 0.60 × 10^9 mol·min^{-1} (mean ± SEM, n = 3). The k_{off} was calculated to be 0.72 ± 0.05 min^{-1} (mean ± SEM, n = 7) and 0.61 ± 0.04 min^{-1} (mean ± SEM, n = 4) using 10 µmol·L^{-1} clobenpropit and GSK1004723 respectively. No significant difference was observed between k_{off} values determined with clobenpropit and GSK1004723 (Student's unpaired *t*-test).

Competition binding studies

In order to determine the affinity of unlabelled antagonists under equilibrium conditions in CHO cell membranes recombinantly expressing either the human H_1 or H_3 receptor, competition displacement binding curves for GSK1004723 (H_1 and H_3), mepyramine (H_1) and GSK189254 (H_3) were measured against [^{3}H]-mepyramine (H_1) or [^{3}H]-GSK189254 (H_3) following a 5 h incubation period at 37°C. The pK_i values determined for GSK1004723, GSK189254 and mepyramine are summarized in Table 1. GSK1004723 was shown to bind with high affinity to both the H_1 and H_3 receptor, with higher affinity for H_3. GSK1004723 caused inhibition of radioligand binding to NSB levels at both receptor subtypes (Figure 2).

Competition kinetic studies

The time taken for a radioligand to reach equilibrium with its receptor is slower in the presence of an unlabelled competitor (Hulme and Birdsall, 1992). Consequently, [^{3}H]-mepyramine takes longer to equilibrate with the H_1 receptor in the presence of an unlabelled H_1 antagonist. Likewise, [^{3}H]-GSK189254 will take longer to equilibrate with the H_3 receptor in the presence of an unlabelled H_3 antagonist. In addition, the kinetic characteristics of the unlabelled antago-

Table 1

H_1 and H_3 receptor affinity values and binding kinetics for unlabelled antagonists

Antagonist	Receptor	k_{on} (mol·min^{-1})	k_{off} (min^{-1})	$t_{1/2}$ (min)	pK_D	pK_i
GSK1004723	H_1	7.33 ± 0.13 × 10^7	0.009 ± 0.002	73	9.91 ± 0.05	10.2 ± 0.24
Mepyramine	H_1	1.11 ± 0.23 × 10^9	0.817 ± 0.046	0.9	9.04 ± 0.10	8.86 ± 0.05
GSK1004723	H_3	4.76 ± 0.69 × 10^8	0.007 ± 0.001	89	10.8 ± 0.12	10.6 ± 0.03
GSK189254	H_3	3.04 ± 0.14 × 10^9	0.802 ± 0.010	0.9	9.58 ± 0.01	9.49 ± 0.07

Derived kinetic values were calculated by globally fitting experimental data generated at 37°C to the Motulsky and Mahan (1984) model. Dissociation $t_{1/2}$ were calculated from k_{off} values and K_D (shown as negative log, pK_D) calculated from k_{off}/k_{on} values as described under *Data analysis and statistics*. K_i (shown as negative log, pK_i) calculated from IC_{50} values determined under equilibrium conditions in competition binding experiments, using Cheng–Prusoff equation, as described under *Data analysis and statistics*. Data are means ± SEM for four separate determinations.

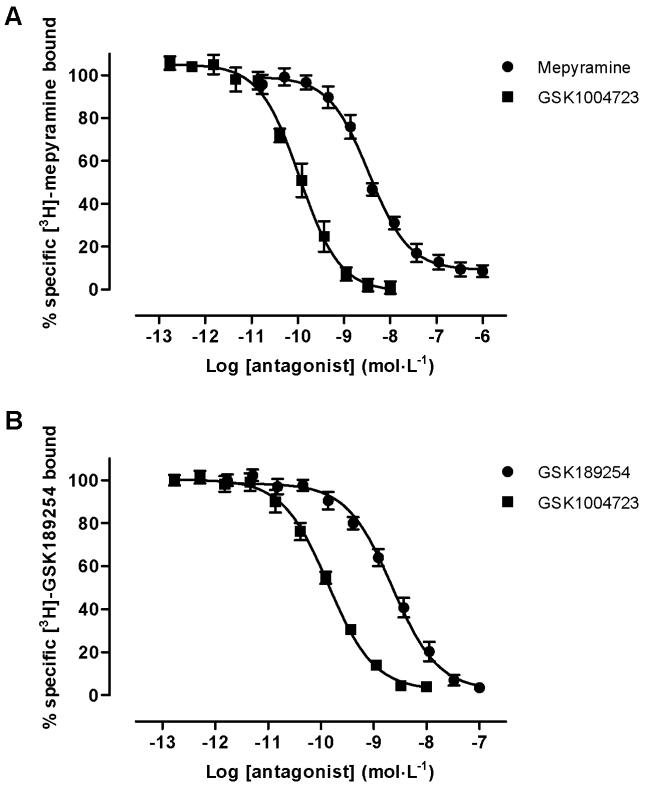

Figure 2

Competition displacement binding curves for (A) mepyramine and GSK1004723 against [^{3}H]-mepyramine in recombinant CHO-H_1 membranes and (B) GSK189254 and GSK1004723 against [^{3}H]-GSK189254 in recombinant CHO-H_3 membranes. Full IC_{50} curves were generated by incubating a range of unlabelled antagonist concentrations with CHO-H_1 membranes and [^{3}H]-mepyramine or CHO-H_3 membranes and [^{3}H]-GSK189254. Plates were filtered after a 5 h incubation at 37°C and the amount of radioligand bound to receptor was measured by liquid scintillation spectroscopy. Non-specific binding values were measured in the presence of 10 μmol·L^{-1} azelastine (H_1) or clobenpropit (H_3) and used to calculate % specific radioligand bound. The competition binding displacement curve data shown are the mean ± SEM of four individual experiments carried out in duplicate.

nist will influence the equilibration time (Motulsky and Mahan, 1984; Dowling and Charlton, 2006). Therefore, the slower the k_{off} of the antagonist from the receptor, the longer it will take the system to reach steady state.

Competition kinetic studies were performed by generating [^{3}H]-mepyramine and [^{3}H]-GSK189254 association curves in the absence and presence of a range of unlabelled antagonists at 37°C. Experimental data at the H_1 receptor were obtained with [^{3}H]-mepyramine, using concentrations of 5, 10 and 20 nmol·L^{-1} for mepyramine (Figure 3A) and 40, 80 and 120 nmol·L^{-1} for GSK1004723 (Figure 3B). Experimental data at the H_3 receptor were obtained with [^{3}H]-GSK189254, using concentrations of 1, 2 and 4 nmol·L^{-1} for GSK189254 (Figure 4A) and 5, 10 and 20 nmol·L^{-1} for GSK1004723 (Figure 4B). Data for an antagonist with a fast dissociation profile (mepyramine/GSK189254) was generated using lower multiples of its K_i (<15 × K_i). However, in order to achieve full resolution of radioligand equilibrium binding in the same experimental incubation time, a slowly dissociating antagonist (GSK1004723) was employed with much greater multiples of K_i (>200 × K_i). For each unlabelled antagonist a k_{on} and k_{off} was calculated in each individual experiment from the global fit of the Motulsky and Mahan (1984) competition kinetics model to the three different antagonist concentrations tested and vehicle. The k_{on} and k_{off} values were then used to calculate the $t_{1/2}$ and K_D values. These data were used to generate the mean ± SEM for the four separate determinations (all kinetically derived parameters shown in Table 1).

The pK_i values determined for all antagonists from competition displacement binding curves at equilibrium were in good agreement with their kinetically derived pK_D. In addition, there was an excellent correlation between the k_{on} and k_{off} values calculated for [^{3}H]-mepyramine and [^{3}H]-GSK189254 from association and dissociation radioligand binding studies and those kinetically derived for the unlabelled forms in competition kinetic studies. These data show that kinetically derived parameters were being calculated robustly by the Motulsky and Mahan (1984) model and allowed comparisons to be drawn between antagonists. Consequently, the k_{off} value for GSK1004723 was shown to be significantly slower than that observed for mepyramine at the H_1 receptor and GSK189254 at the H_3 receptor (Student's unpaired *t*-test, $P < 0.001$).

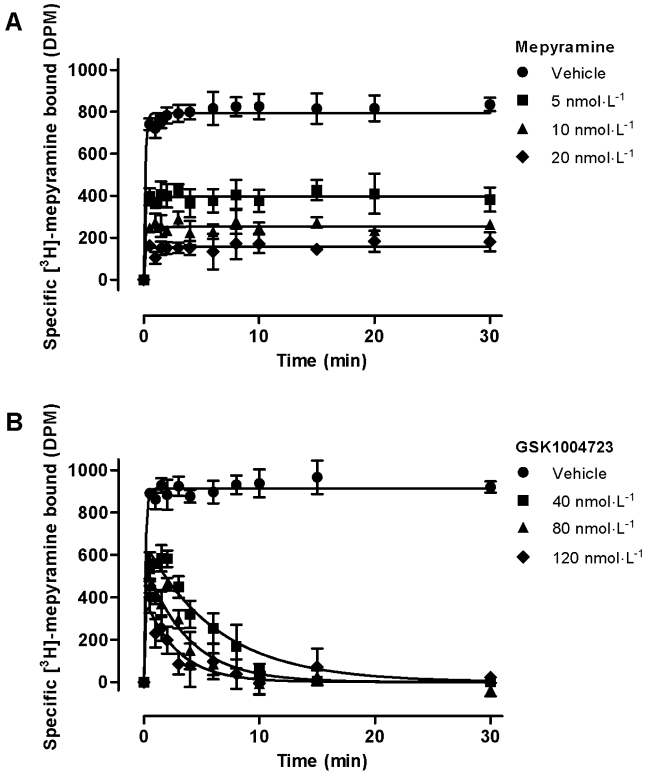

Figure 3

Competition kinetic curves for [^{3}H]-mepyramine in either the absence or presence of (A) mepyramine (5, 10 and 20 nmol·L^{-1}) or (B) GSK1004723 (40, 80 and 120 nmol·L^{-1}) in recombinant CHO-H_1 membranes. Association binding curves for [^{3}H]-mepyramine were generated by incubating radioligand with CHO-H_1 membranes and unlabelled antagonist/vehicle at 37°C. Plates were filtered at the time points indicated and the amount of radioligand bound to receptor was measured by liquid scintillation spectroscopy. Non-specific binding values were measured in the presence of 10 µmol·L^{-1} azelastine and used to calculate specific radioligand bound. Data were fitted to the Motulsky and Mahan, (1984) model, as described under *Data analysis and statistics*, with k_{on} and k_{off} values for unlabelled antagonists derived (summarized in Table 1). Data shown are the mean ± SEM of quadruplicate points and are representative of four individual experiments with similar results. DPM, disintegrations per minute.

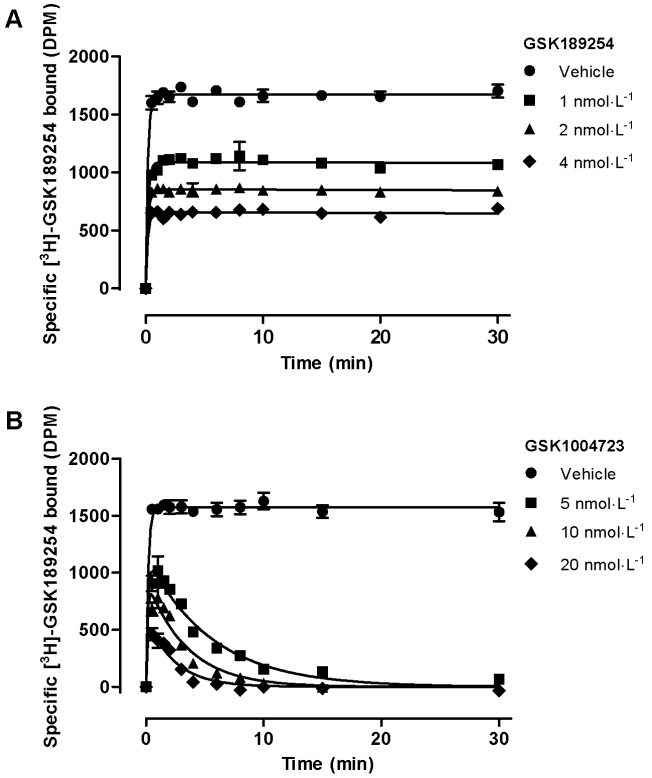

Figure 4

Competition kinetic curves for [^{3}H]-GSK189254 in either the absence or presence of (A) GSK189254 (1, 2 and 4 nmol·L^{-1}) or (B) GSK1004723 (5, 10 and 20 nmol·L^{-1}) in recombinant CHO-H_3 membranes. Association binding curves for [^{3}H]-GSK189254 were generated by incubating radioligand with CHO-H_3 membranes and unlabelled antagonist/vehicle at 37°C. Plates were filtered at the time points indicated and the amount of radioligand bound to receptor was measured by liquid scintillation spectroscopy. Non-specific binding values were measured in the presence of 10 µmol·L^{-1} clobenpropit and used to calculate specific radioligand bound. Data were fitted to the Motulsky and Mahan, (1984) model, as described under *Data analysis and statistics*, with k_{on} and k_{off} values for unlabelled antagonists derived (summarized in Table 1). Data shown are the mean ± SEM of quadruplicate points and are representative of four individual experiments with similar results. DPM, disintegrations per minute.

Histamine receptor selectivity

The selectivity of GSK1004723 for H_1 and H_3 over the other histamine receptor subtypes (H_2 and H_4) was established by testing the ability of GSK1004723 to block either histamine-evoked cAMP production (H_2) or [^{3}H]-histamine binding (H_4) in membranes prepared from HEK293 cells recombinantly over-expressing the human form of the receptor at ambient room temperature (20–22°C). GSK1004723 was demonstrated to be highly selective for H_1 and H_3 receptors (Table 2) demonstrating at least a 15 000-fold selectivity for H_1 and H_3 versus H_2 and H_4.

Antagonism of functional responses mediated by human recombinant H_1 and H_3 receptors

In CHO-K1 cells over-expressing the human H_1 receptor, histamine caused concentration related increases in intracellular Ca^{2+} at 37°C. GSK1004723 showed no evidence for agonist activity in this test system (data not shown) and antagonized the effect of histamine, causing concentration dependent rightward displacement of the histamine CRC (Figure 5A). Some suppression of the maximum response to histamine was also observed at higher concentrations of GSK1004723. GSK1004723 (10–100 nmol·L^{-1}) had no effect in this test system on the responses to Ca^{2+} ionophore, ionomycin, or the endoplasmic reticulum Ca^{2+} ATPase inhibitor, thapsigargin, demonstrating the molecule was not antagonizing histamine via a non-specific effect (data not shown).

A pA_2 value of 8.29 ± 0.11 (mean ± SEM, n = 6) and Schild slope of 1.75 (1.37, 2.14) (mean with 95% confidence intervals in parentheses, n = 6) were estimated for GSK1004723 indicating that at the short incubation time used (30 min) in these experiments GSK1004723 was not at equilibrium. In

Table 2

GSK1004723 selectivity at human recombinant histamine receptors

	Human histamine receptor H_1	H_2	H_3	H_4
Test system	CHO-K1 membranes	HEK293 membranes	CHO-K1 membranes	HEK293 membranes
Assay format	Radioligand binding	cAMP production	Radioligand binding	Radioligand binding
Affinity estimate	pK_i = 10.2 ± 0.24 (n = 4)	$pIC_{50} \leq 5.1$ (n = 2)	pK_i = 10.6 ± 0.03 (n = 4)	$pIC_{50} \leq 6.0$ (n = 2)

K_i (shown as negative log, pK_i) calculated from IC_{50} values determined under equilibrium conditions in competition binding experiments, using Cheng–Prusoff equation, as described under *Data analysis and statistics*. Data for H_1/H_3 are means ± SEM for four separate determinations. Competition binding experiments were carried out at 37°C for H_1/H_3 and ambient room temperature (20–22°C) for H_2/H_4.

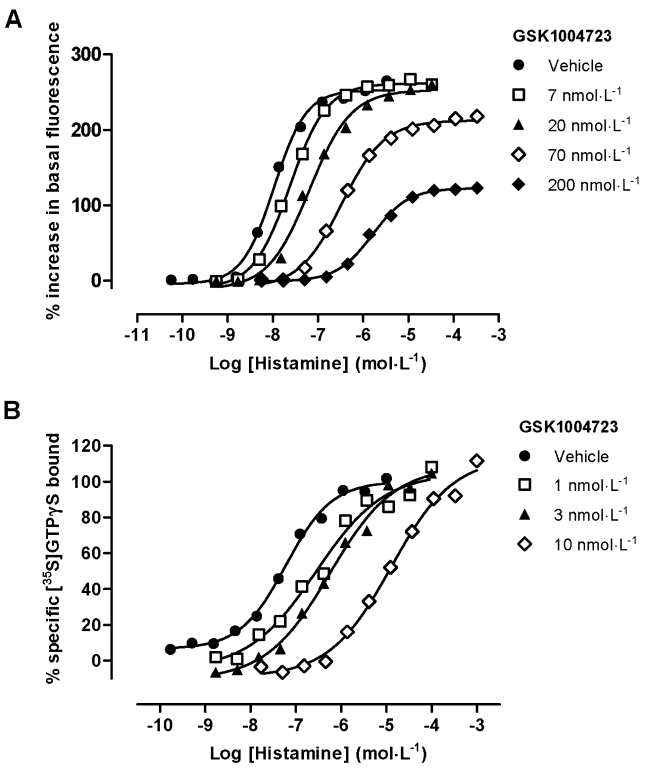

Figure 5

The antagonism profile for GSK1004723 at human recombinant H_1 and H_3 receptors. Histamine-induced increases in intracellular Ca^{2+} in CHO cells expressing human H_1 receptors (A) following a 30 min incubation in either vehicle or increasing concentrations of GSK1004723 at 37°C. Histamine-induced increases in [^{35}S]GTPγS binding in CHO cells expressing human H_3 receptors (B) following a 30 min incubation in either vehicle or increasing concentrations of GSK1004723 at 30°C. Data shown are a single experiment representative of four to six individual experiments with similar results.

additional studies, increasing the GSK1004723 incubation time to 4 h resulted in an increase in pA_2 to 8.89 ± 0.10 and a Schild slope of 1.42 (0.90, 1.95) (mean with 95% confidence intervals in parentheses, n = 6) (data not shown). This Schild slope was still greater than unity and suggests that GSK1004723 requires incubation times in excess of 4 h to reach equilibrium in this test system.

In CHO-K1 membranes, generated from cells over-expressing human H_3 receptors, histamine-induced a concentration dependent increase in [^{35}S]GTPγS binding at 30°C. GSK1004723 antagonized histamine causing concentration dependent rightward displacement of the histamine CRC with no reduction in the maximum response (Figure 5B). Schild analysis on data generated following a 30 min incubation period yielded a slope greater than unity of 1.38 (1.05, 1.70) (mean with 95% confidence intervals in parentheses, n = 4) and a pA_2 of 9.71 ± 0.31 (mean ± SEM, n = 4) was calculated. GSK1004723 had no effect on basal [^{35}S]GTPγS binding in the absence of histamine showing a lack of agonist activity at the human H_3 receptor (data not shown).

Duration of antagonism of responses mediated by human recombinant H_1 and H_3 receptors

To generate antagonist inhibition curves, cells were exposed to various concentrations of antagonist and then stimulated 30 min later with a single submaximal concentration of histamine to stimulate increases in intracellular Ca^{2+} (Figure 6) at 37°C. To explore the duration of antagonism, prior to histamine challenge some cells were washed after exposure to antagonist and allowed to re-equilibrate (3 and 4.5 h for CHO-H_1 and CHO-H_3 cells respectively) prior to histamine challenge.

In cells expressing H_1 receptors (Figure 6A), GSK1004723 caused a concentration dependent antagonism of the histamine response as did the H_1 receptor antagonist, mepyramine. However, in cells washed and allowed to re-equilibrate following exposure to antagonist, almost complete loss of mepyramine-induced antagonism was observed with no loss of antagonism to GSK1004723 (Figure 6A). Similarly, in cells expressing H_3 receptors (Figure 6B), GSK1004723 caused a concentration dependent antagonism of the histamine response as did the H_3 receptor antagonist, clobenpropit. However, in cells washed and allowed to re-equilibrate following exposure to antagonist, almost complete loss of clobenpropit-induced antagonism was observed with only a small rightward displacement of the GSK1004723 inhibition curve (Figure 6B).

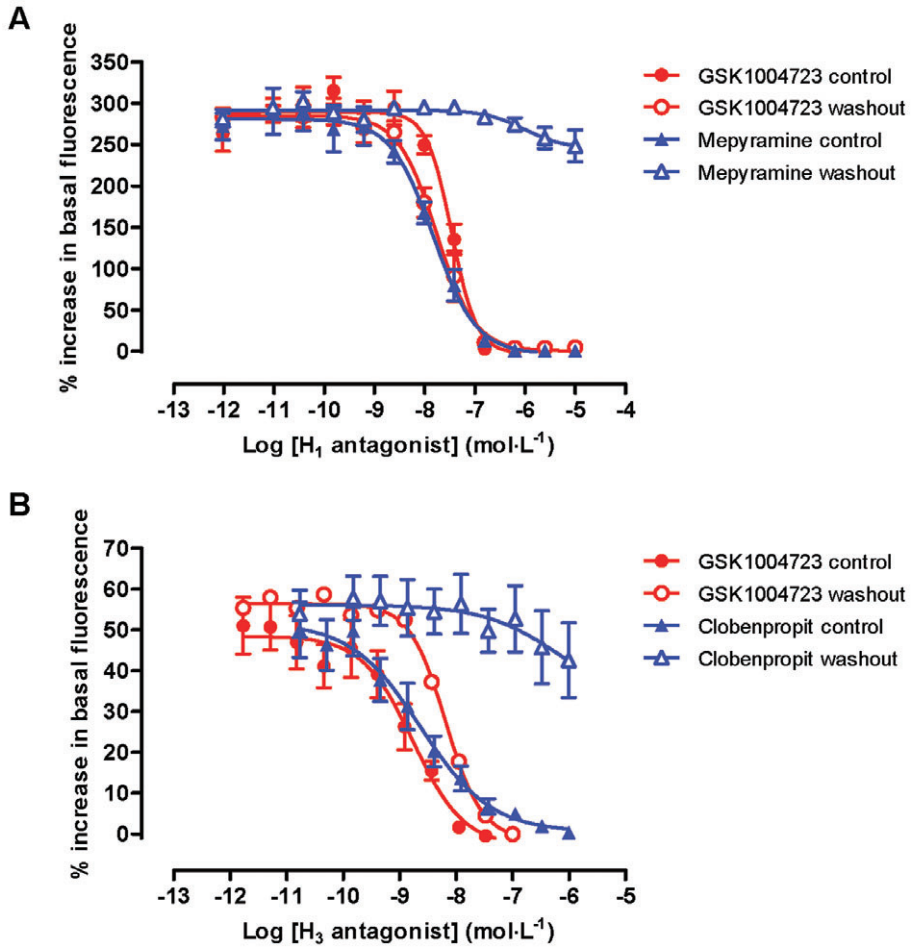

Figure 6

Duration of antagonism at human recombinant H_1 and H_3 receptors. CHO cells expressing either H_1 receptors (A) or H_3 receptors (B) were exposed to various concentrations of GSK1004723, the H_1 receptor antagonist mepyramine or the H_3 receptor antagonist clobenpropit and then stimulated 30 min later with a single submaximal concentration of histamine to stimulate increases in intracellular Ca^{2+} at 37°C. To explore the duration of antagonism, prior to histamine challenge some cells were washed after exposure to antagonist and allowed to re-equilibrate (3 and 4.5 h for CHO-H_1 and CHO-H_3 cells respectively) prior to histamine challenge. Data shown are the mean ± SEM of six individual experiments.

Duration of antagonism of responses mediated by endogenously expressed H_1 receptors

The duration of antagonism of GSK1004723 versus responses mediated by human endogenous H_1 receptors was explored using superfused preparations of human isolated bronchus. The duration of action was compared to mepyramine, a classical selective H_1 receptor antagonist with a short duration of action, and azelastine, a selective and long-lasting H_1 receptor antagonist which is approved for clinical use as a once or twice a day intranasal treatment for rhinitis. Experiments were conducted with equi-effective concentrations of antagonist (100 nmol·L^{-1}).

The addition of histamine (10 μmol·L^{-1}) to the superfusate perfusing the bronchi produced a rapid and sustained contraction [mean contraction at plateau = 1.96 ± 0.21 g (mean ± SEM, n = 4)]. In the continuing presence of histamine, the antagonists were then superfused over the tissue resulting in a reversal of the histamine-induced contraction. All the antagonists caused almost a complete reversal of the histamine-induced tone (data not shown). Mepyramine produced the most rapid effect with a mean $t_{1/2}$ of 11 min relative to 30 min for azelastine and 63 min for GSK1004723. Three hours post-antagonist perfusion, when the response had reached a plateau, they were removed from the perfusate and the rate of recovery from the effect of the antagonist was assessed. Figure 7A demonstrates that rapid recovery was observed from the effects of the short-lasting antagonist, mepyramine, with almost full recovery of histamine-induced tone observed within 2 h of removal of the antagonist from the Kreb's solution perfusing the tissue. In contrast, azelastine induces a more sustained antagonism (Figure 7A) and 10 h post-removal of azelastine from the perfusate, there was approximately 40% recovery of the histamine-induced contractile response. Similarly, GSK1004723 also displayed a sustained duration of action (Figure 7A) such that 10 h post-removal of GSK1004723 from the perfusate, there was still

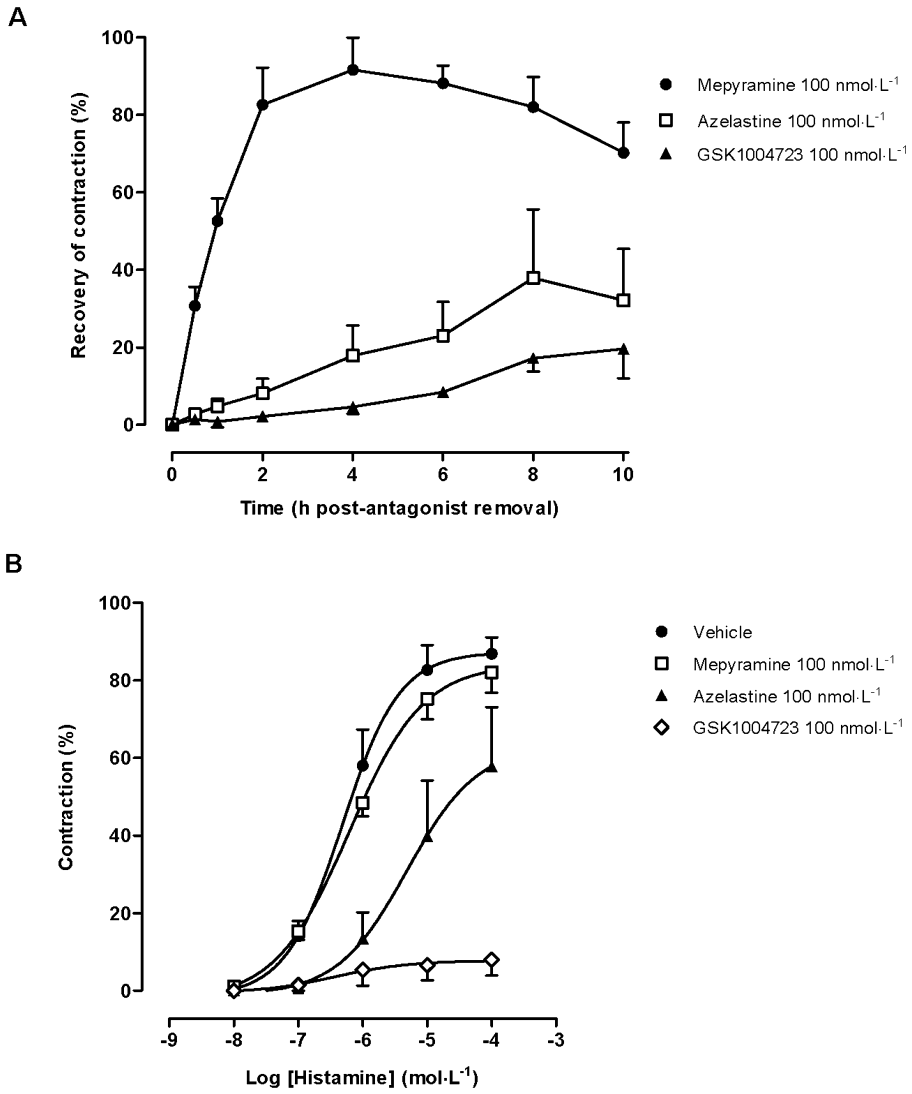

Figure 7

Duration of functional H_1 receptor antagonism measured by histamine-mediated contraction in isolated human bronchus superfusion tissue baths. The recovery of histamine-induced contraction (A) was measured over a 10 h period post-removal of antagonist (azelastine, GSK1004723 or mepyramine at 100 nmol·L^{-1}) from perfusate. Histamine-mediated smooth muscle contraction (B) was measured in either the absence or presence of antagonists (azelastine, GSK1004723 or mepyramine at 100 nmol·L^{-1}) following a 21 h washout (removal of antagonist/vehicle from the perfusate). Recovery of histamine-induced contraction data are expressed as a percentage of the initial antagonist inhibition of contraction. Histamine concentration response curve data are expressed as a percentage of the final carbachol-induced contraction. Data shown are the mean (+ or − SEM for clarity) of three to four individual experiments using tissues from separate lung donors.

greater than 80% inhibition of the histamine-induced response. The following day, approximately 19 h after antagonist removal from the perfusate, histamine was removed from the perfusate. Preparations were then allowed to re-equilibrate. At this point, approximately 21 h post-antagonist removal, the preparations were again exposed to histamine and a CRC constructed. This data indicated that in tissues which had been previously incubated with GSK1004723 on the preceding day, responses to histamine were still completely antagonized (Figure 7B) although the tissues remained responsive to carbachol (data not shown) confirming tissue viability and specificity of antagonism. Tissues which had been exposed to the long-lasting H_1 antagonist azelastine, also displayed some degree of apparent residual antagonism with an approximate 10-fold rightward displacement of the histamine CRCs. In contrast, there was no evidence of sustained antagonism in bronchial preparations which had been exposed to mepyramine (Figure 7B).

Duration of antagonism of responses in the guinea pig following intranasal compound treatment and challenge: whole body plethysmography

Intranasal instillation of histamine caused a significant increase in PenH over the 40 min recording period. PenH has

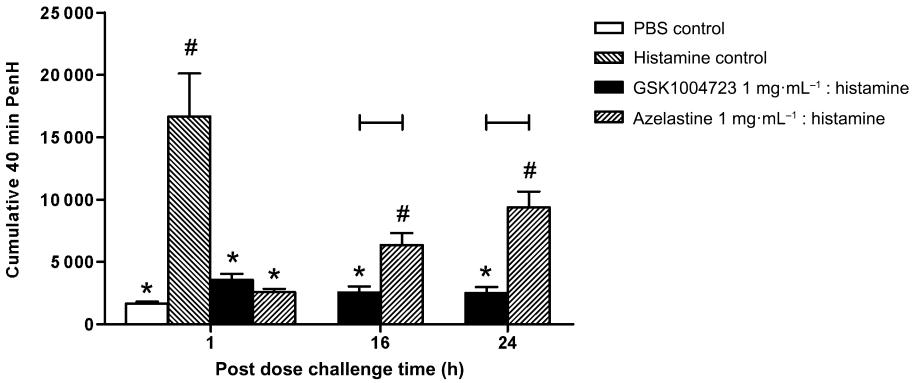

Figure 8

Azelastine and GSK1004723 duration of antagonism *in vivo*. Guinea pigs were pre-dosed with either saline, GSK1004723 or azelastine (for 1 h, 16 h or 24 h) prior to 15 mmol·L^{-1} histamine or phosphate buffered saline (PBS) challenge. Cumulative enhanced pause (PenH) was recorded during 40 min in whole body plethysmography chambers and displayed as mean ± SEM of six to 10 individual animals. PenH values deemed to be statistically different from histamine control shown as * and from PBS control # with bars representing all other relevant and significant comparisons (Hochberg analysis on $\log_{10}$ transformed data, $P < 0.05$).

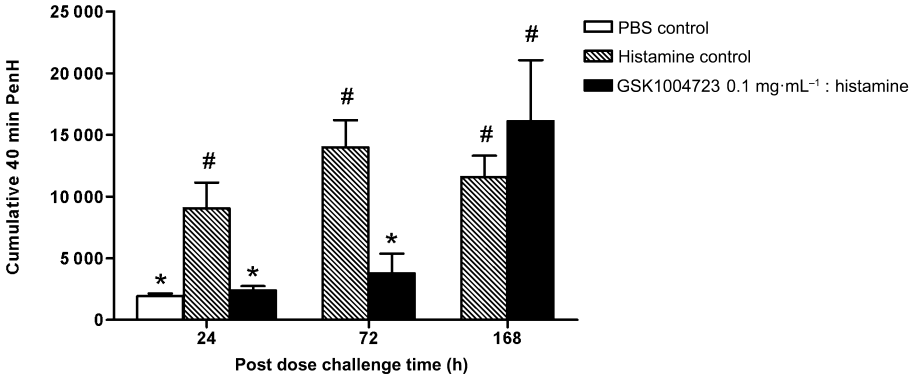

Figure 9

GSK1004723 extended duration of antagonism *in vivo*. Guinea pigs were pre-dosed with either saline or GSK1004723 (24 h, 72 h or 168 h) prior to 15 mmol·L^{-1} histamine or phosphate buffered saline (PBS) challenge. Cumulative enhanced pause (PenH) was recorded during 40 min in whole body plethysmography chambers and displayed as mean ± SEM of six to 10 individual animals. PenH values deemed to be statistically different from time-matched histamine control shown as * and from PBS control # (Hochberg analysis on $\log_{10}$ transformed data, $P < 0.05$).

been described in the literature as a suitable surrogate marker of airway occlusion (Hamelmann *et al.*, 1997; Saunders *et al.*, 2007). Both azelastine and GSK1004723 were able to significantly inhibit the nasal response to 15 mmol·L^{-1} histamine when they were dosed at 1 mg·mL^{-1}, 1 h before challenge. GSK1004723 was able to maintain inhibition for 24 h, while azelastine lost significance when dosed 16 h or 24 h prior to the challenge (Figure 8). At a 10-fold lower dose, GSK1004723 was also able to significantly inhibit the response to histamine when dosed either 24 h or 72 h prior to the histamine challenge, but was no longer effective when dosed 168 h (7 days) in advance of challenge (Figure 9).

Discussion

Although often trivialized as a disease, allergic rhinitis continues to impact quality of life for millions of patients worldwide and also carries a significant economic burden (Schoenwetter *et al.*, 2004; Borres, 2009). While effective treatment options do exist, including intranasal corticosteroids and histamine H_1 receptor antagonists (intranasal and oral), all current treatment options fall short of an optimal profile in terms of efficacy and convenience (Meltzer *et al.*, 2010). A large range of histamine H_1 receptor antagonists are available to physicians and patients. Although many of these antihistamines have a rapid onset of action, once a day dosing and reasonably manage the symptoms of rhinorrhoea, sneezing and itching, they fall short in dealing with the troublesome symptom of nasal congestion (Spector, 1999; Meltzer *et al.*, 2010). Therefore, there is a need for novel, convenient treatments which can provide better control of all of the symptoms of allergic rhinitis. Emerging literature based on clinical (Taylor-Clark and Foreman, 2005; Taylor-Clark *et al.*, 2005) and non-clinical (McLeod *et al.*, 1999) data points to a role for the histamine H_3 receptor in histamine-

induced nasal congestion and suggests that combined H_1 and H_3 receptor antagonism has the potential to provide patients with relief from all the key symptoms of rhinitis, including nasal congestion. Consequently, we initiated a drug discovery programme to identify a novel, potent, dual H_1 and H_3 receptor antagonist with a long duration of action, consistent with once a day intranasal dosing to patients. GSK1004723 is the clinical candidate arising from that drug discovery programme and this manuscript describes some of the key non-clinical pharmacological characteristics of this interesting molecule.

Characterization of the affinity and receptor kinetics of GSK1004723 was carried out using human recombinant histamine receptors. Our radioligand binding studies, carried out at both the H_1 and H_3 receptor, are consistent with GSK1004723 having a high affinity at both receptor subtypes and an approximate fourfold higher affinity for the H_3 receptor over the H_1 receptor.

At both receptors, GSK1004723 inhibited radioligand binding to NSB levels and when used to calculate radioligand dissociation the k_{off} value was not significantly different to that measured with a competitive antagonist. This behaviour is consistent with a competitive rather than a non-competitive, allosteric mode of action (Christopoulos and Kenakin, 2002). In-depth analysis of H_1 and H_3 receptor kinetics using the competition kinetics method described by Motulsky and Mahan (1984) allowed the accurate determination of k_{on} and k_{off} values for GSK1004723 and then from these, K_D and receptor dissociation $t_{1/2}$-values were derived. The K_D values agree well with the pK_i values from the competition binding curves. The dissociation $t_{1/2}$-values show that GSK1004723 exhibits slow dissociation kinetics from the H_1 and H_3 receptor. Throughout these binding studies GSK1004723 has shown the characteristics of a slowly reversible antagonist at both the H_1 and H_3 receptor, with no evidence of a non-competitive interaction at either receptor. Furthermore, additional studies using membrane fragments generated from cells expressing human recombinant H_2 and H_4 receptors indicate that GSK1004723 demonstrates a high degree of selectivity (at least 15 000-fold) for H_1 and H_3.

The same human recombinant H_1 and H_3 receptor expressing cell lines used in the binding studies were also used to confirm the ability of GSK1004723 to antagonize the effects of histamine and to explore duration of antagonism. The data indicate that GSK1004723 acts as a potent antagonist at both human H_1 and H_3 receptors. There is no evidence of partial agonist activity against either of these receptors. GSK1004723-induced antagonism of H_1 and H_3 mediated responses appears to be specific because no antagonism of responses to other stimuli (ionomycin, thapsigargin) were observed. The suppression of the maximum response to histamine, observed at high concentrations of GSK1004723-induced antagonism of H_1 receptors, is indicative of either a lack of temporal equilibrium with a slowly dissociating orthosteric antagonist or an allosteric interaction (Kenakin *et al.*, 2006). In radioligand competition binding studies, GSK1004723 showed no evidence of an allosteric interaction with either the H_1 or H_3 receptor. In addition, from radioligand competition kinetic studies it has been shown to slowly dissociate from both receptors. Therefore, these observations, combined with the steep Schild curves in the functional H_1 studies with a 30 min incubation period, strongly suggest that the suppression of the maximum response is due to hemi-equilibrium conditions rather than an allosteric interaction. Therefore, these experiments using human recombinant receptors confirm that GSK1004723 is a potent, dual H_1 and H_3 receptor antagonist. In terms of duration of action in this cell based system, GSK1004723 behaved as a long-acting antagonist of responses mediated by both H_1 and H_3 receptors. This was demonstrated by showing that in cells exposed to increasing concentrations of GSK1004723, washing of the cells prior to histamine challenge followed by either a 3 h (H_1) or 4.5 h (H_3) re-equilibration did not markedly inhibit the GSK1004723-induced antagonism of the histamine response. In contrast, this washing and re-equilibration procedure completely abolished the effects of the short-lasting H_1 antagonist, mepyramine, and the short-lasting H_3 antagonist, clobenpropit.

Having demonstrated that GSK1004723 was a potent and long-lasting antagonist of human recombinant H_1 and H_3 receptors in cell culture, we next wanted to determine whether a similar profile would be observed when studying responses to histamine in a native expression system. Therefore, for these experiments we used continually superfused human isolated bronchi to study the dynamics of GSK1004723-induced antagonism of H_1 mediated contractile responses. These studies of duration of antagonism in human tissue focused on the H_1 receptor as despite significant efforts we were unable to establish a suitable system to carry out similar studies versus H_3 mediated responses. The superfused human bronchus studies produced data consistent with the studies on human recombinant H_1 receptors demonstrating that once established the antagonist effect of GSK1004723 is sustained for at least 21 h and is difficult to reverse. The long-lasting antagonism displayed by GSK1004723 appeared to be specific since the preparations were still sensitive to the muscarinic agonist, carbachol. Contrasting with GSK1004723, the short-lasting H_1 antagonist mepyramine behaved as anticipated, with almost complete recovery of histamine-induced contractions in the 10 h period post-antagonist removal. For context, the potent and long-acting H_1 selective receptor antagonist, azelastine, was also studied. Azelastine is approved for the treatment of rhinitis in Europe and the USA and a once a day formulation was recently granted a license in the USA (van Bavel *et al.*, 2009). In this human bronchus assay, azelastine also produced long-lasting antagonism of histamine-induced contractile responses. However, the duration of action appeared less than GSK1004723 since at 21 h post-antagonist removal although residual antagonism was still apparent, histamine CRCs were only approximately 10-fold to the right of those observed in vehicle treated preparations.

These latter *in vitro* experiments focused both on human recombinant and endogenous histamine receptors, providing good evidence that GSK1004723 is a long-acting H_1 and H_3 receptor antagonist. The observation that GSK1004723 has a longer duration of action than azelastine in superfused bronchi is consistent with the hypothesis that it has the potential to have a once a day clinical duration of action. To further test that hypothesis, a series of *in vivo* experiments were carried out, again in comparison with the clinically approved once or twice a day antihistamine, azelastine. These experi-

ments again focused on duration of antagonism at H_1 receptors since despite significant efforts we have been unable to establish a non-clinical *in vivo* model suitable for profiling duration of antagonist action at H_3 receptors. Duration of action of GSK1004723 *in vivo* was evaluated using a conscious guinea pig model in which intranasal histamine evokes a reduction in nasal airspace (Saunders *et al.*, 2007). Antagonists can be administered intranasally at various time points prior to histamine challenge to follow their ability to block the histamine response and determine their duration of action. In this model, intranasal azelastine completely blocks the histamine response acutely (1 h post-azelastine); however, by 16 h it no longer significantly inhibits the histamine-induced response. This is consistent with clinical experience where azelastine is given either as a once or twice a day treatment, depending on dose. In contrast to azelastine, intranasal pretreatment with GSK1004723 at comparable or lower doses to azelastine produced effective antagonism of histamine-induced responses for up to 3 days post-antagonist administration. Therefore, both *in vitro* and *in vivo*, GSK1004723 displays a very long-lasting blockade of H_1 receptors. Unfortunately, despite significant efforts, we were unable to establish a suitable model in which to test the duration of GSK1004723-induced antagonism of H_3 mediated responses *in vivo*, so the question of whether the molecule can achieve the same long duration of H_3 antagonism *in vivo* as was demonstrated for H_1 mediated responses is one that would benefit from clinical or further non-clinical investigations.

What are the key factors responsible for the long duration of action of GSK1004723? The radioligand binding kinetic data suggest that its duration of action is in part a consequence of the high affinity of the molecule for H_1 and H_3 receptors coupled to slow dissociation. However, it is likely that the physicochemical characteristics of GSK1004723 also contribute to its pharmacological profile and longevity of antagonism. Therefore, GSK1004723 is a dibasic, lipophilic molecule, and it has been reported for other molecules that both these features are likely to favour partitioning into lipid membranes and prolonged activity of interaction with G-protein coupled receptors (Anderson, 1993; Austin *et al.*, 2003). Consequently, a reasonable working hypothesis is that a combination of high receptor affinity, slow receptor dissociation, and the ability to preferentially partition into biological membranes, best explains the pharmacological behaviour of GSK1004723. This hypothesis is consistent with relatively slow equilibration, the resistance of GSK1004723 to reversal by washing in cells and tissue *in vitro*, and its long duration of action *in vivo*.

In conclusion, the *in vitro* and *in vivo* data for GSK1004723 are consistent, showing that it is a novel, potent and selective dual H_1 and H_3 receptor antagonist. Moreover, GSK1004723 displays a prolonged duration of action at H_1 and H_3 receptors *in vitro* and at the H_1 receptor *in vivo*. This pharmacological profile is consistent with the potential for once a day intranasal dosing of GSK1004723 in allergic rhinitis.

Acknowledgements

The authors would like to acknowledge the entire scientific and management team at GlaxoSmithKline that contributed to the discovery, characterization and progression of GSK1004723.

Conflicts of interest

All authors are currently or have been full-time employees of GlaxoSmithKline.

References

Al Suleimani YM, Walker MJA (2007). Allergic rhinitis and its pharmacology. Pharmacol Ther 114: 233–260.

Alexander SP, Mathie A, Peters JA (2009). Guide to Receptors and Channels (GRAC), 4th edn. Br J Pharmacol 158 (Suppl. 1): S1–S254.

Anderson GP (1993). Formoterol: pharmacology, molecular basis of agonism, and mechanism of long duration of a highly potent and selective beta 2-adrenoceptor agonist bronchodilator. Life Sci 52: 2145–2160.

Arrang JM, Garbarg M, Schwartz JC (1983). Auto-inhibition of brain histamine release mediated by a novel class (H_3) of histamine receptor. Nature 302: 832–837.

Arunlakshana O, Schild HO (1959). Some quantitative uses of drug antagonists. Br J Pharmacol Chemother 14: 48–58.

Austin RP, Barton P, Bonnert RV, Brown RC, Cage PA, Cheshire DR *et al.* (2003). QSAR and the rational design of long-acting dual D_2-receptor/β_2-adrenoceptor agonists. J Med Chem 46: 3210–3220.

van Bavel J, Howland WC, Amar NJ, Wheeler W, Sacks H (2009). Efficacy and safety of azelastine 0.15% nasal spray administered once daily in subjects with seasonal allergic rhinitis. Allergy Asthma Proc 30: 512–518.

Borres MP (2009). Allergic rhinitis: more than just a stuffy nose. Acta Paediatr 98: 1088–1092.

Bradford MM (1976). A rapid and sensitive method for the quantitation of microgram quantities of protein utilizing the principle of protein-dye binding. Anal Biochem 72: 248–254.

Cheng Y, Prusoff WH (1973). Relationship between the inhibition constant (K_i) and the concentration of inhibitor which causes 50 per cent inhibition (IC_{50}) of an enzymatic reaction. Biochem Pharmacol 22: 3099–3108.

Christopoulos A, Kenakin T (2002). G-protein-coupled receptor allosterism and complexing. Pharmacol Rev 55: 323–374.

Coleman RA, Nials AT (1989). Novel and versatile superfusion system. Its use in the evaluation of some spasmogenic and spasmolytic agents using guinea-pig isolated tracheal smooth muscle. J Pharmacol Methods 21: 71–86.

Dowling MR, Charlton SJ (2006). Quantifying the association and dissociation rates of unlabelled antagonists at the muscarinic M_3 receptor. Br J Pharmacol 148: 927–937.

Gillard M, Chatelain P (2006). Changes in pH differently affect the binding properties of histamine H_1 receptor antagonists. Eur J Pharmacol 530: 205–214.

Hamelmann E, Schwarze J, Takeda K, Oshiba A, Larsen GL, Irvin CG (1997). Noninvasive measurement of airway responsiveness in allergic mice using barometric plethysmography. Am J Respir Crit Care Med 156: 766–775.

Hill AV (1909). The mode of action of nicotine and curari, determined by the form of the contraction curve and the method of temperature coefficients. J Physiol 39: 361–373.

Howarth PH (1997). Mediators of nasal blockage in allergic rhinitis. Allergy 52 (Suppl. 40): 12–18.

Hulme EC, Birdsall NJM (1992). Strategy and tactics in receptor-binding studies. In: Hulme EC (ed.). Receptor-Ligand Interactions – A Practical Approach. Oxford: IRL Press, pp. 63–176.

Kenakin T, Jenkinson S, Watson C (2006). Determining the potency and molecular mechanism of action of insurmountable antagonists. J Pharmacol Exp Ther 319: 710–723.

Kost TA, Condreay JP (2002). Recombinant baculoviruses as mammalian cell gene-delivery vectors. Trends Biotechnol 20: 173–180.

Leurs R, Bakker RA, Timmerman H, de Esch IJP (2005). The histamine H_3 receptor: from gene cloning to H_3 receptor drugs. Nat Rev Drug Discov 4: 107–120.

Liu C, Wilson SJ, Kuei C, Lovenberg TW (2001). Comparison of human mouse, rat and guinea-pig histamine H_4 receptors reveals substantial pharmacological species variation. J Pharmacol Exp Ther 299: 121–130.

Lovenberg TW, Roland BL, Wilson SJ, Jiang X, Pyati J, Huvar A *et al*. (1999). Cloning and functional expression of the human histamine H_3 receptor. Mol Pharmacol 55: 1101–1107.

McLeod RL, Mingo GG, Herczku C, DeGennaro-Culver F, Kreutner W, Egan RW *et al*. (1999). Combined histamine H_1 and H_3 receptor blockade produces nasal decongestion in an experimental model of nasal congestion. Am J Rhinol 13: 391–399.

Medhurst AD, Atkins AR, Beresford IJ, Brackenborough B, Briggs MA, Calver AR *et al*. (2007). GSK189254, a novel H_3 receptor antagonist that binds to histamine H_3 receptors in alzheimer's disease brain and improves cognitive performance in preclinical models. J Pharmacol Exp Ther 321: 1032–1045.

Meltzer EO, Caballero F, Fromer LM, Krouse JH, Scadding G (2010). Treatment of congestion in upper respiratory diseases. Int J Gen Med 3: 69–91.

Motulsky HJ, Mahan LC (1984). The kinetics of competitive radioligand binding predicted by the law of mass action. Mol Pharmacol 25: 1–9.

Nakaya M, Takeuchi N, Kondo K (2004). Immunohistochemical localization of histamine receptor subtypes in human inferior turbinates. Ann Otol Rhinol Laryngol 113: 552–557.

Passalacqua G, Ciprandi G (2006). Novel therapeutic interventions for allergic rhinitis. Expert Opin Investig Drugs 15: 1615–1625.

Saunders KA, Hodgson ST, Ford AJ (2007). The use of whole body plethysmography to assess efficacy and duration of intranasal H_1 antagonists in a guinea pig model of nasal congestion. Am J Respir Crit Care Med 175: A199.

Schoenwetter WF, Dupclay L Jr, Appajosyula S, Botteman MF, Pashos CL (2004). Economic impact and quality-of-life burden of allergic rhinitis. Curr Med Res Opin 20: 305–317.

Smit MJ, Timmerman H, Hijzelendoorn JC, Fukui H (1996). Regulation of the human histamine H_1 receptor stably expressed in Chinese hamster ovary cells. Br J Pharmacol 117: 1071–1080.

Spector S (1999). Pathophysiology and pharmacotherapy of allergic rhinitis. (Foreword). J Allergy Clin Immunol 103: S377.

Taylor-Clark T, Foreman J (2005). Histamine-mediated mechanisms in the human nasal airway. Curr Opin Pharmacol 5: 214–220.

Taylor-Clark T, Sodha R, Warner B, Foreman J (2005). Histamine receptors that influence blockage of the normal human nasal airway. Br J Pharmacol 144: 867–874.

Varty LM, Gustafson E, Laverty M, Hey JA (2004). Activation of histamine H_3 receptors in human nasal mucosa inhibits sympathetic vasoconstriction. Eur J Pharmacol 484: 83–89.

Wood-Baker R, Lau L, Howarth PH (1996). Histamine and the nasal vasculature: the influence of H_1 and H_2-histamine receptor antagonism. Clin Otolaryngol Allied Sci 21: 348–352.